

SWMF Solar/Helio

*Bart van der Holst, I.V. Sokolov,
W.B. Manchester, G. Toth and T.I. Gombosi*





■ New solar corona and inner heliosphere model with low-frequency Alfvén wave turbulence

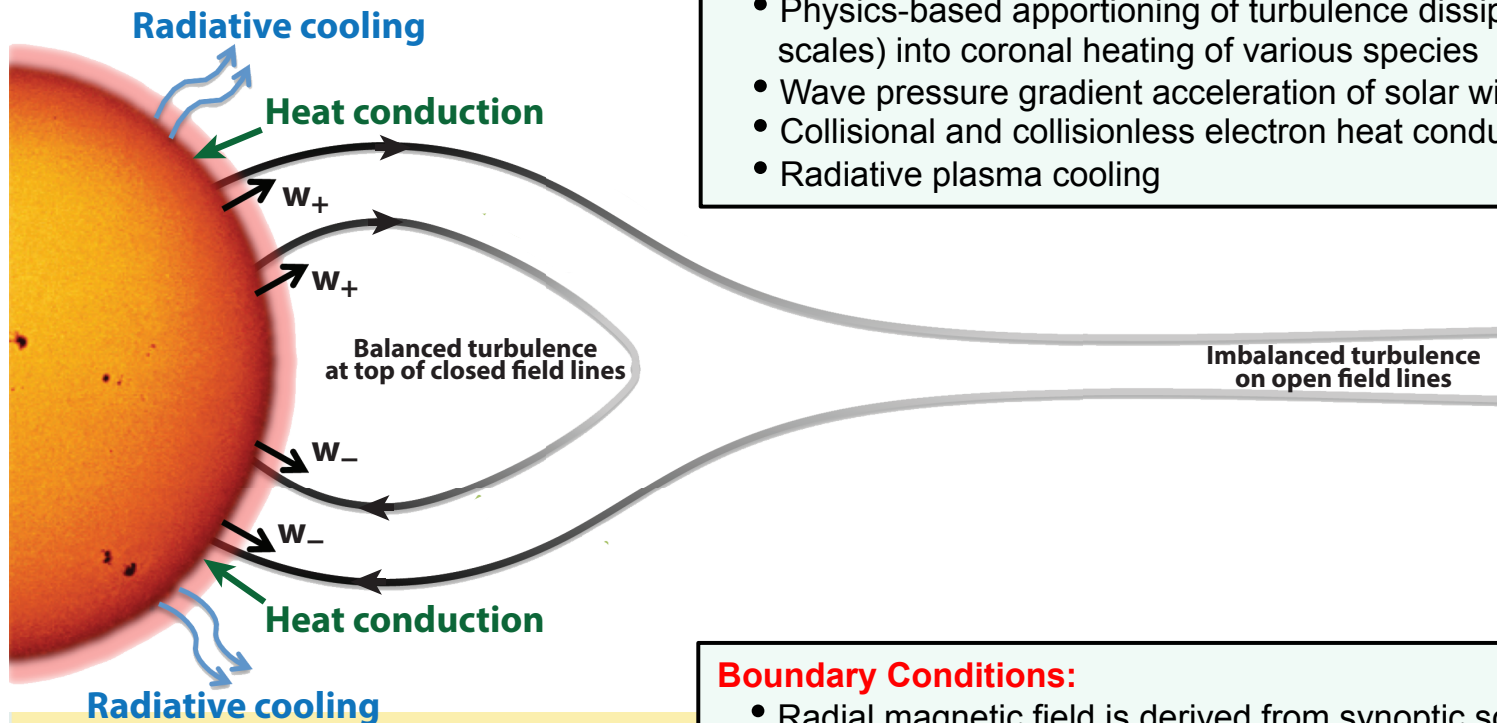
- Physics included in this model
- Validation: EUV images
- Temperature anisotropy and plasma instabilities
- Validation: 1AU in-situ
- Validation: Charge state

■ CMEs

■ Magnetic flux emergence and regional models

Alfvén Wave Solar Model (AWSOM)

B. van der Holst et al. ApJ **782**, 81 (2014).
 R. Oran et al. ApJ **778**, 176 (2013).
 I. Sokolov et al. **764**, 23 (2013).



XMHD physics:

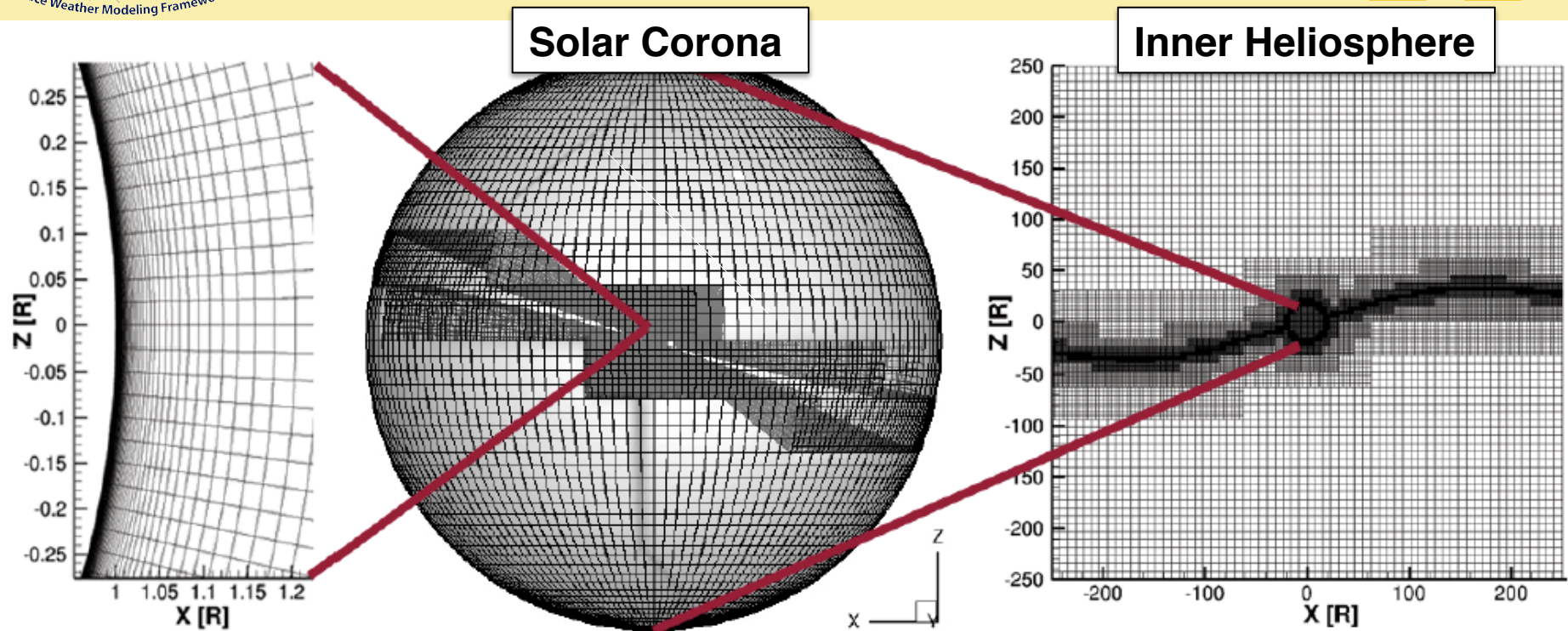
- Separate $T_{p\parallel}$, $T_{p\perp}$ and T_e
- WKB equations for parallel and antiparallel propagating turbulence (w_\pm)
- Non-WKB physics-based reflection of w_\pm results in turbulent cascade
- Correction for presumed uncorrelated waves w_\pm in the balanced turbulence near apex of closed field lines
- Physics-based apportioning of turbulence dissipation (at the gyro-radius scales) into coronal heating of various species
- Wave pressure gradient acceleration of solar wind plasma
- Collisional and collisionless electron heat conduction
- Radiative plasma cooling

Boundary Conditions:

- Radial magnetic field is derived from synoptic solar magnetograms
- Poynting flux of outward propagating turbulence:

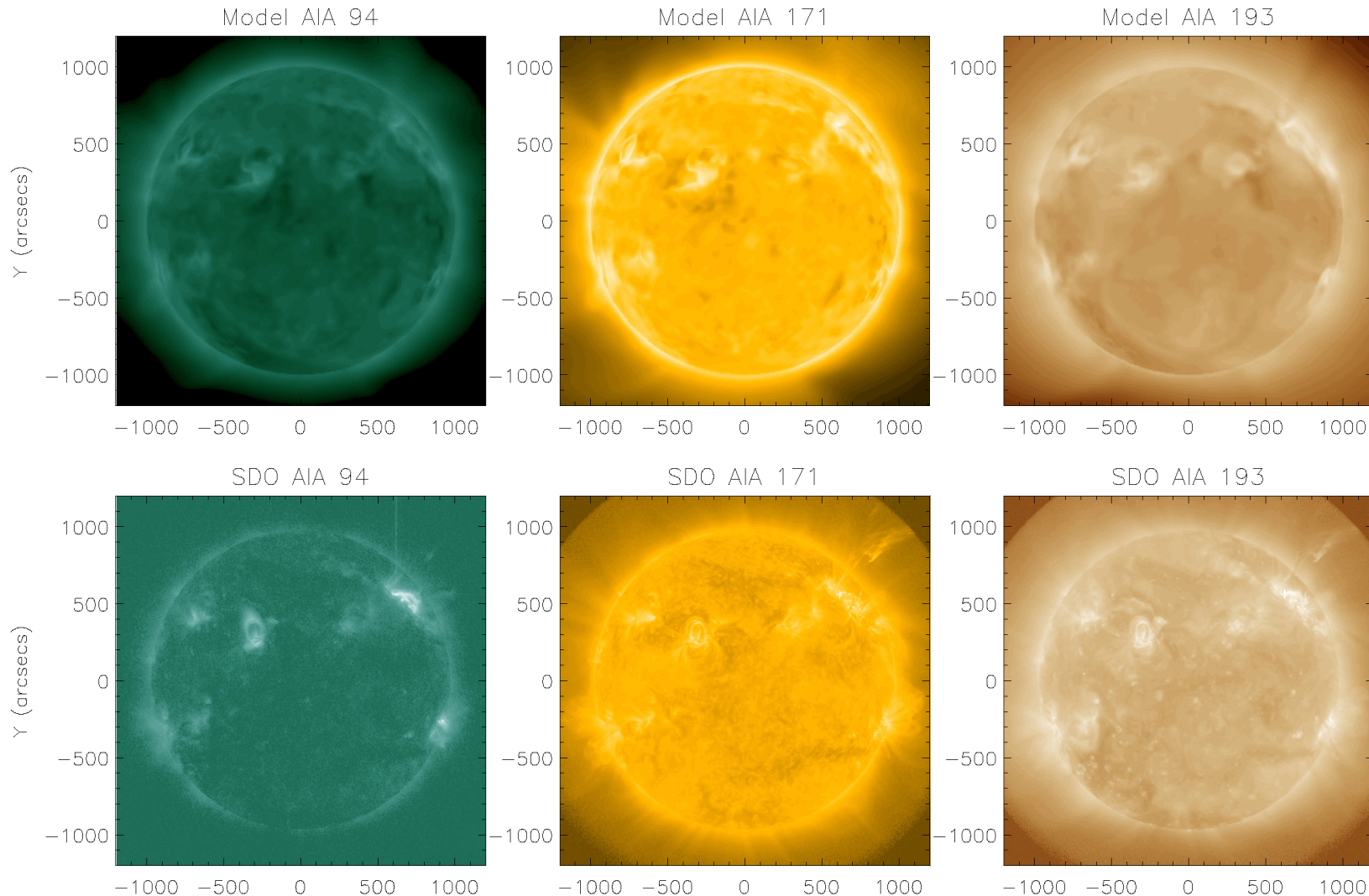
$$(S_A / B) = 1.1 \times 10^6 \text{ W m}^{-2} \text{ T}^{-1}$$

Computational Grids

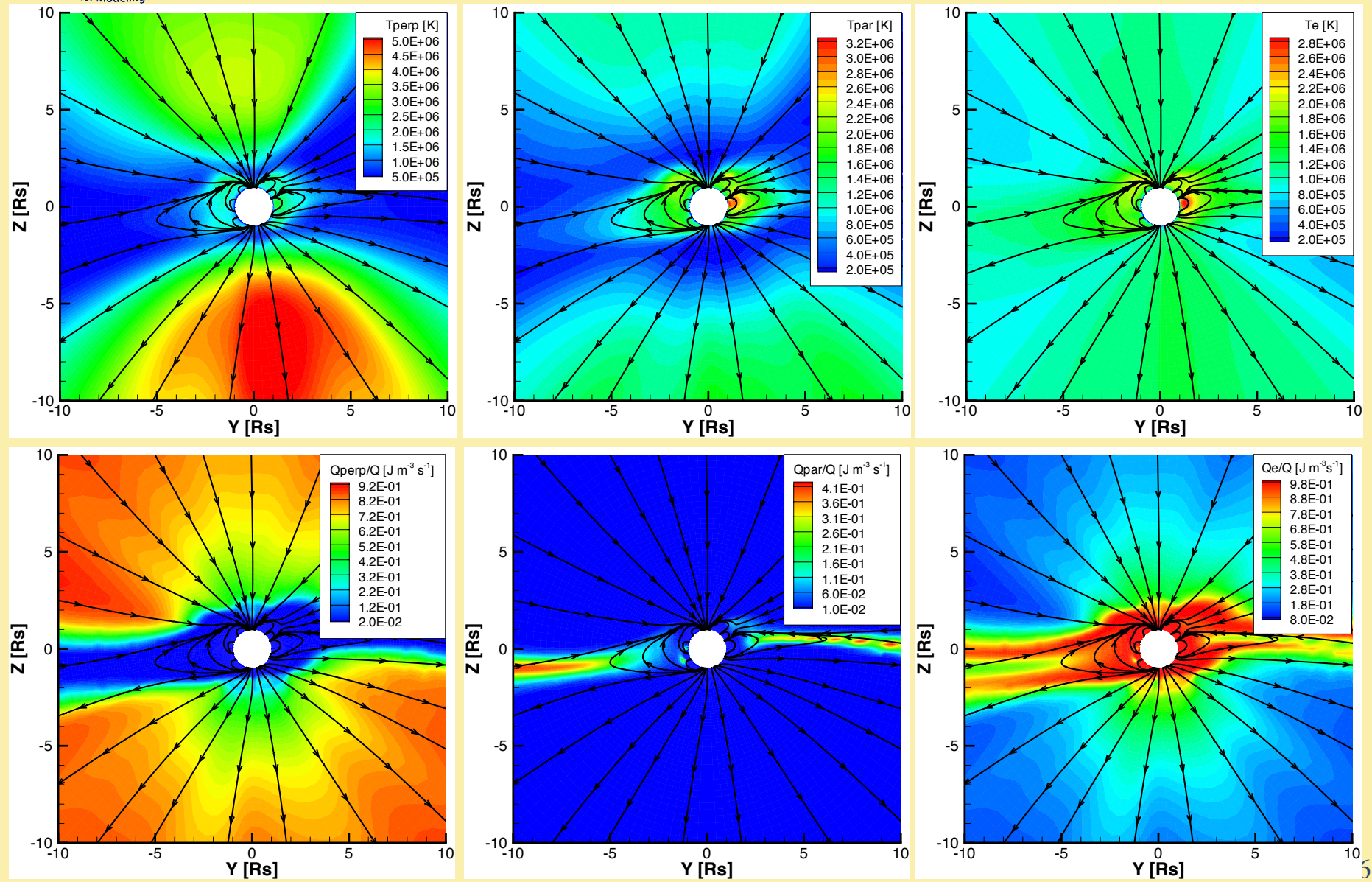


- AWSOM is split in two coupled framework components: stretched spherical grid for solar corona, cartesian grid for inner heliosphere
- Significant grid stretching to grid resolve the upper chromosphere and transition region in addition to artificial transition region broadening (Lionello et al. 2009, Sokolov et al. 2013)
- AMR to resolve the heliospheric currentsheet

Validation: EUV Images for CR2107



Heat Partitioning for the Electron and Anisotropic Proton Temperatures



Limiting the Anisotropic Pressure

X. Meng et al. 2012 JCP, JGR

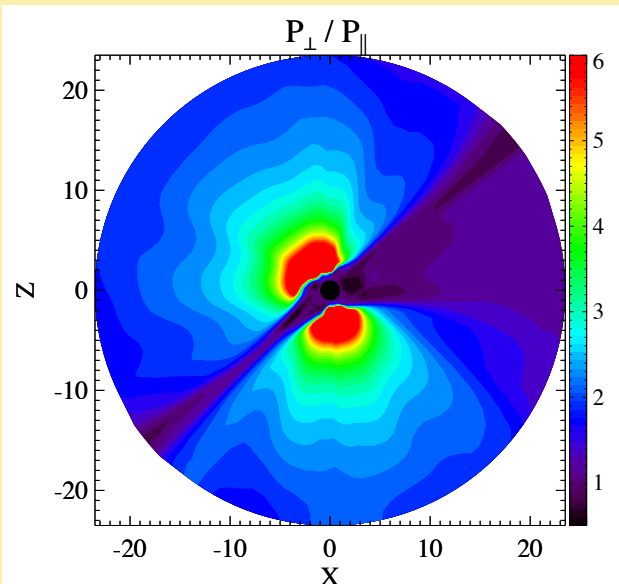
The instability-based anisotropic pressure relaxation towards the marginal stable pressure \bar{p}_{\parallel} while keeping averaged pressure p unmodified:

$$\frac{\delta p_{\parallel}}{\delta t} = \frac{\bar{p}_{\parallel} - p_{\parallel}}{\tau}$$

applied in firehose, mirror and proton cyclotron unstable regions. τ is taken to be the inverse of the growth rates of the instabilities (Hall 1979, 1980, 1981 and Southwood & Kivelson 1993):

	instability criteria	relaxation time τ
firehose	$\frac{p_{\parallel}}{p_{\perp}} > 1 + \frac{\mathbf{B}^2}{\mu_0 p_{\perp}}$	$\tau_f = \frac{1}{\gamma_{fFLR}(\lambda_f)} = \frac{2}{\Omega_i} \frac{\sqrt{p_{\parallel}(p_{\perp} - p_{\parallel}/4)}}{\Delta p_f}$
mirror	$\frac{p_{\perp}}{p_{\parallel}} > 1 + \frac{\mathbf{B}^2}{2\mu_0 p_{\perp}}$	$\tau_m = \frac{1}{\gamma_m(\lambda_m)} = \frac{3\sqrt{5}}{4\Omega_i} \sqrt{\frac{p_{\parallel}}{2\Delta p_m}}$
proton cyclotron	$\frac{p_{\perp}}{p_{\parallel}} > 1 + 0.3 \sqrt{\frac{\mathbf{B}^2}{2p_{\parallel}}}$	$\tau_{ic} = \frac{10^2}{\Omega_i}$

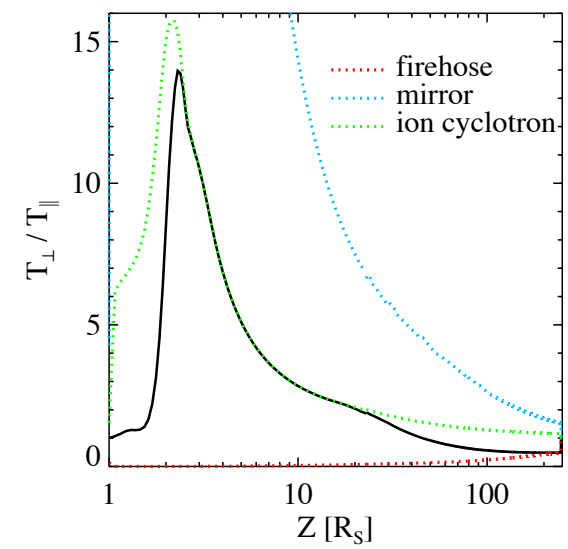
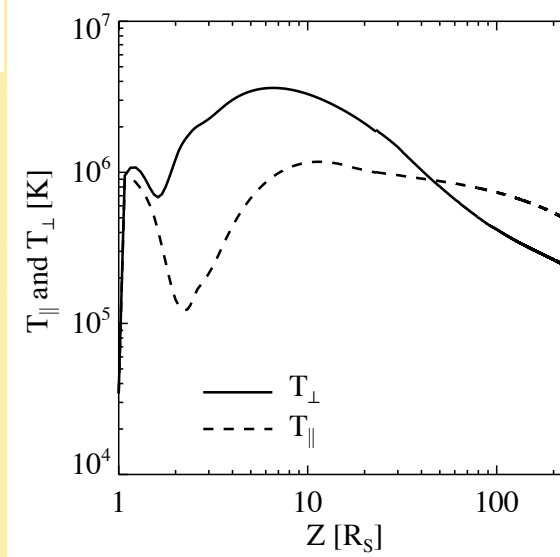
AWSoM with Temperature Anisotropy



M Temperature Anisotropy along the north axis

X. Meng et al., submitted to ApJ

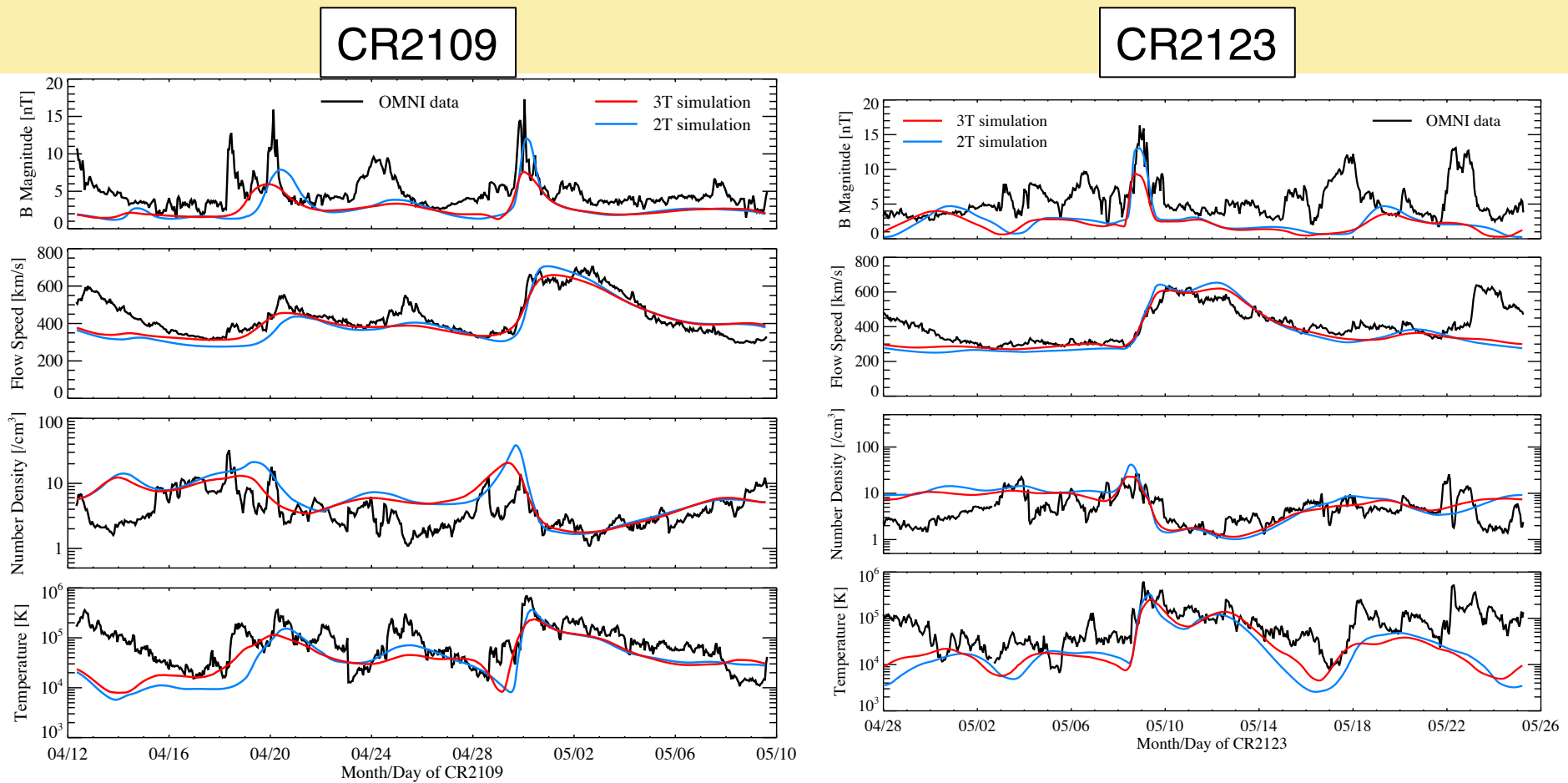
M Temperature anisotropy in the simulated Y=0 meridional slice



Validation at 1AU



ACE versus 2T and 3T models

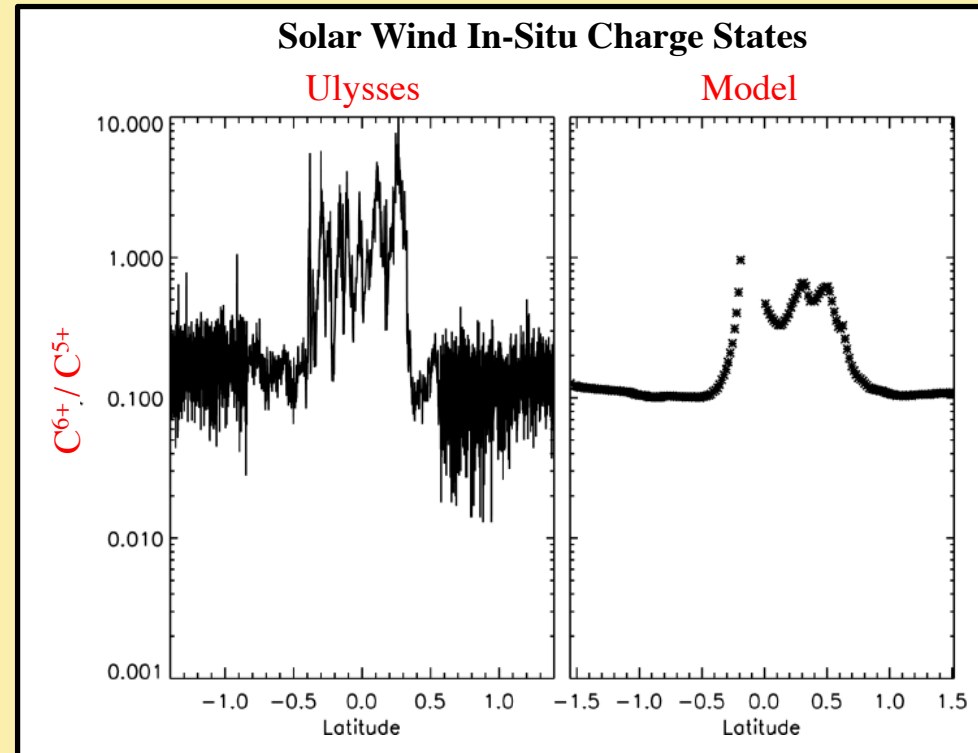
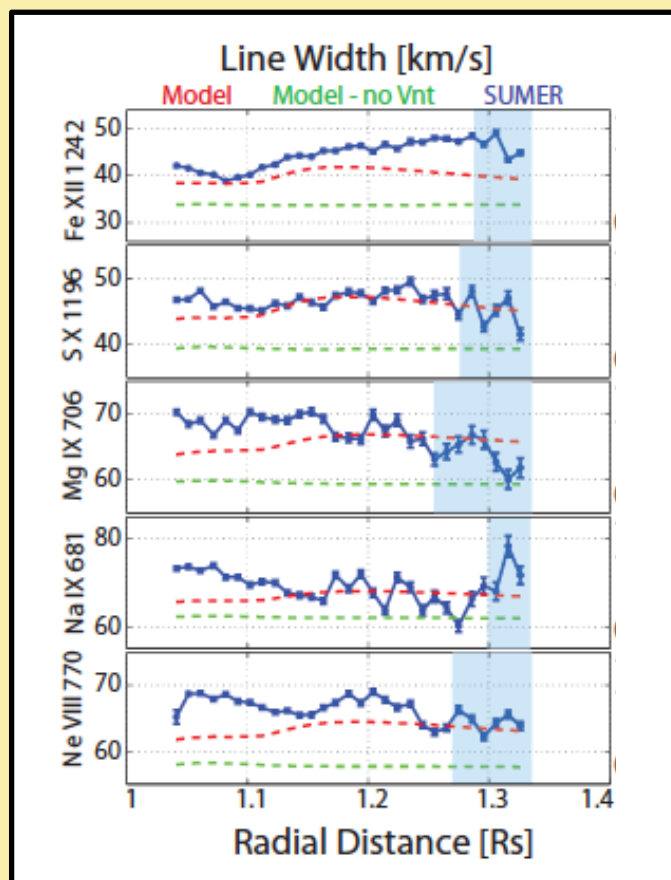


Validation: Charge State



R. Oran et al., submitted to ApJ

M The electron density, temperature and speed from the MHD model are used to drive charge state evolution along field lines, and compared to in-situ and remote observations



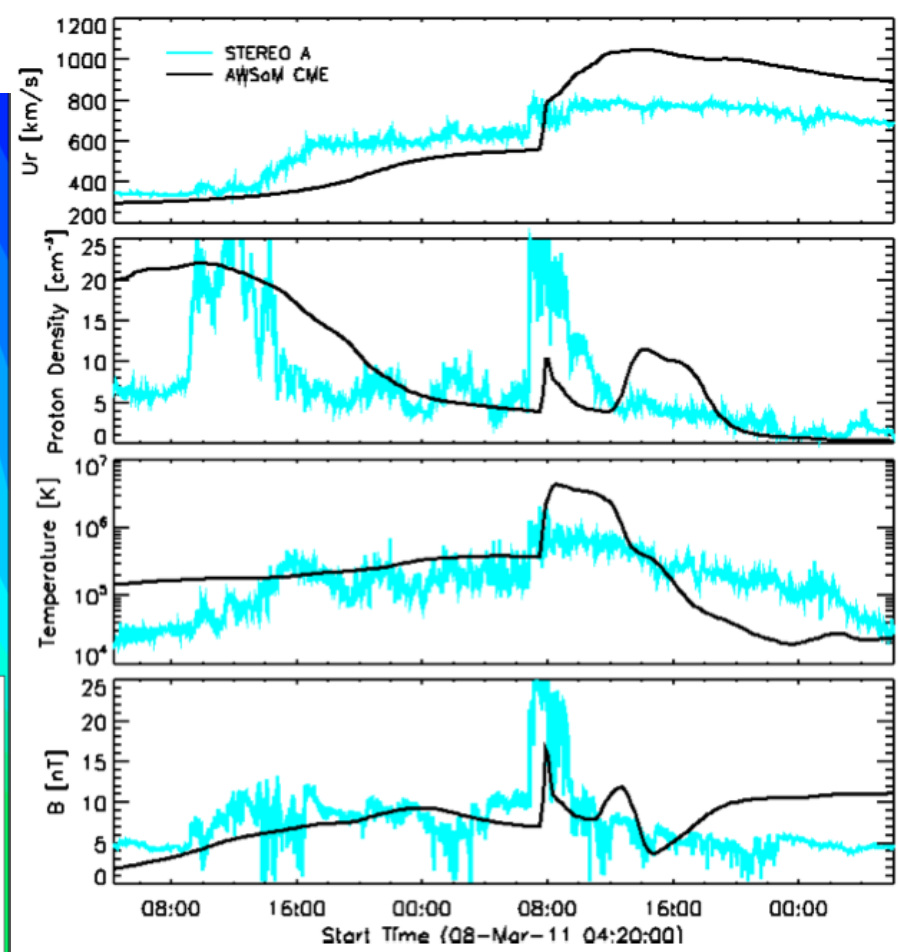
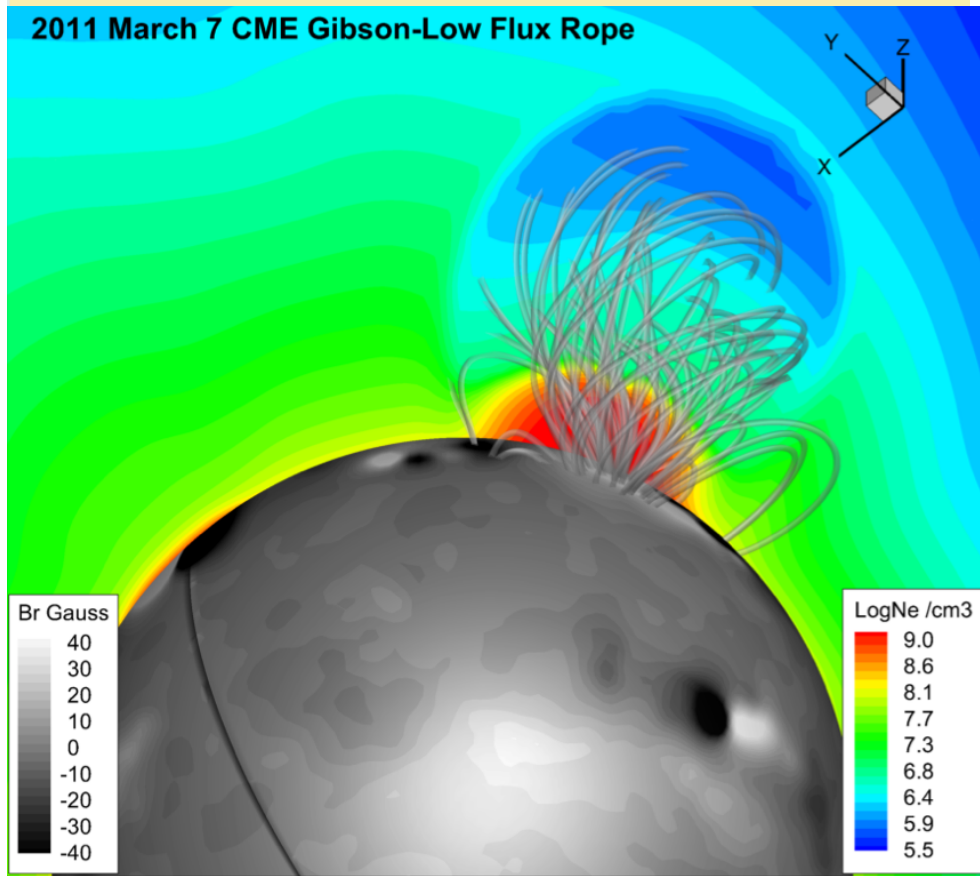
March 7th 2011 CME Simulation



CME simulation with the AWSOM model:

- Gibson-Low flux rope erupts from active region 11164
- Model produces 3 part density of CME progenitors: dense streamer with low density cavity containing a dense core
- SIR-CME interaction crucial to CME structure at 1AU

M. Jin et al. in preparation



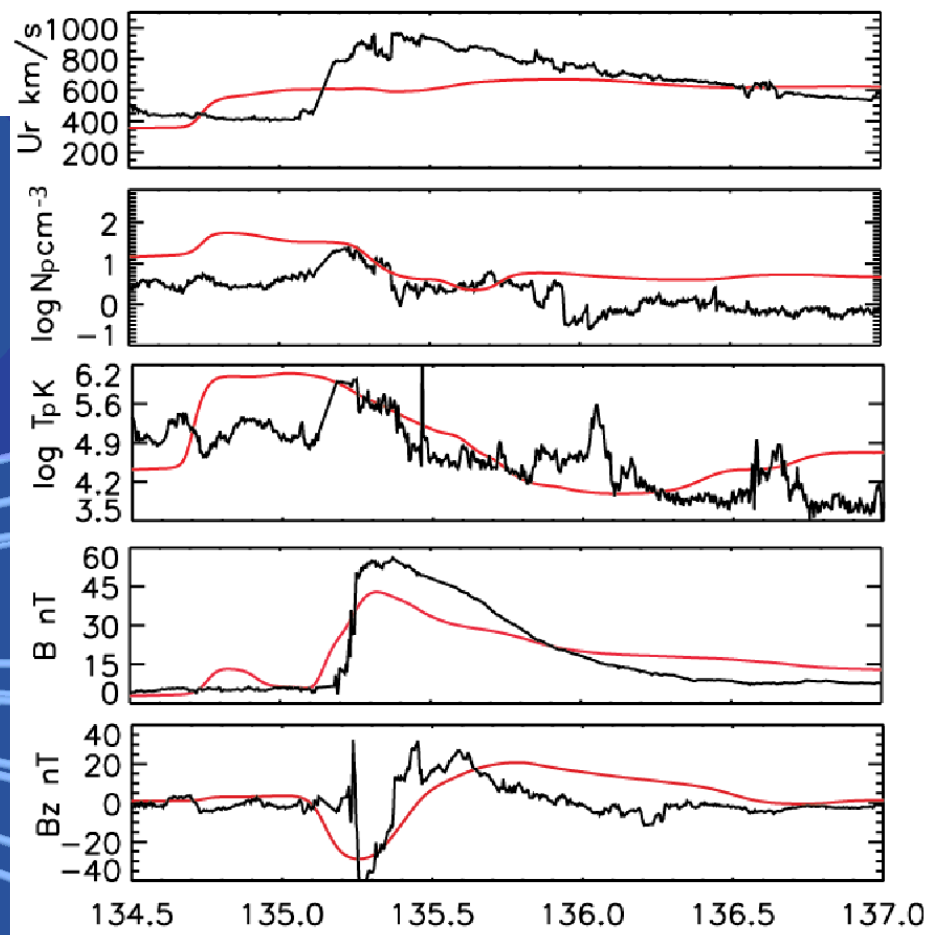
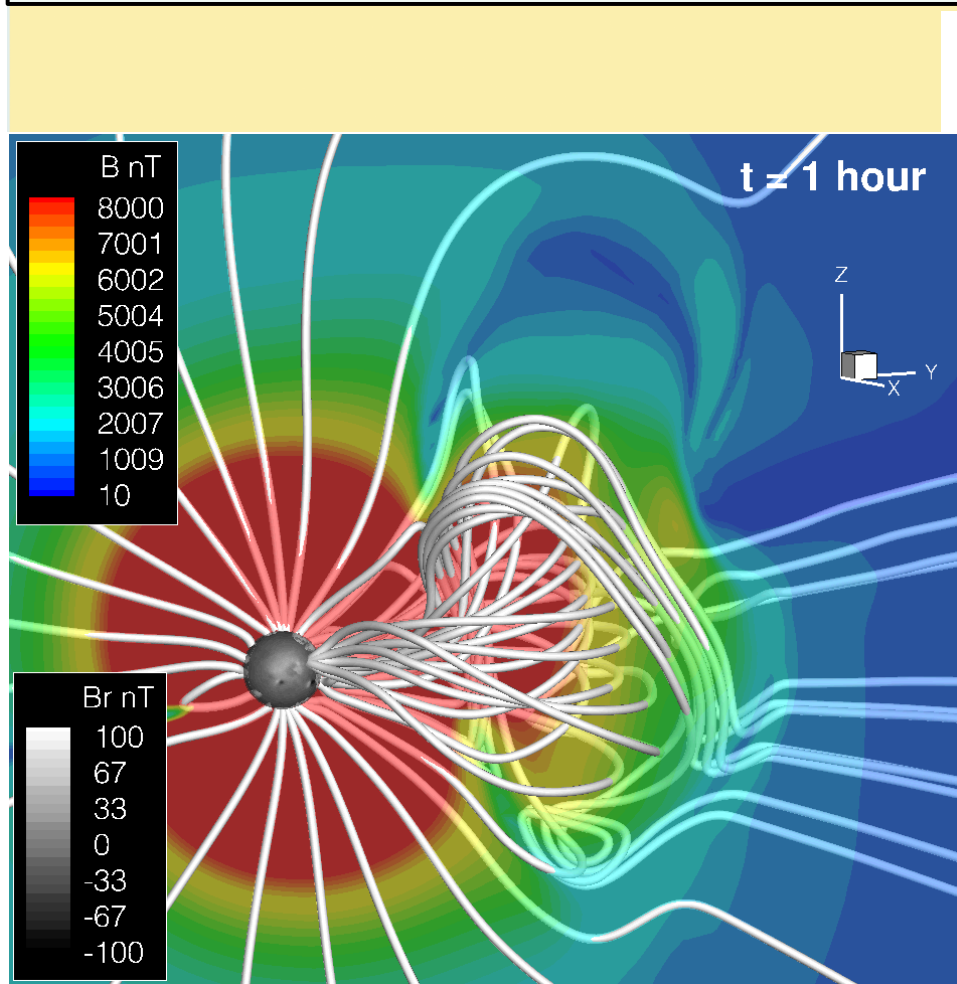
May 13th 2005 CME Simulation



CME Simulation with the AWSoM Model:

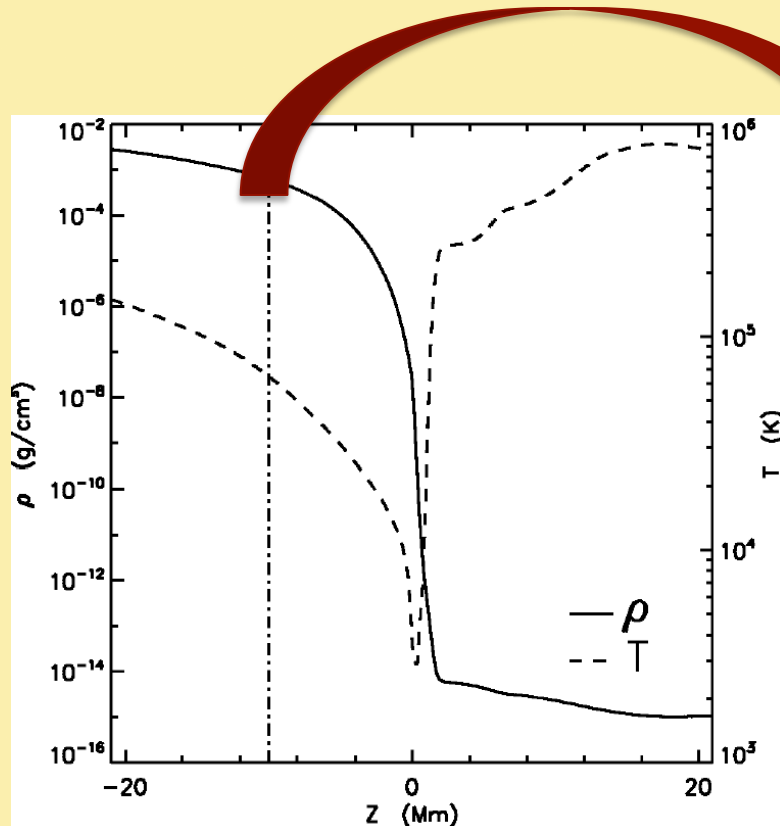
- Gibson-Low flux rope erupts from active region 10759
- The simulation reproduces the magnetic cloud signatures at 1 AU including the B_z rotation.

Manchester, van der Holst & Lavraud,
Plasma Phys. Control. Fusion, 56, 2014 .

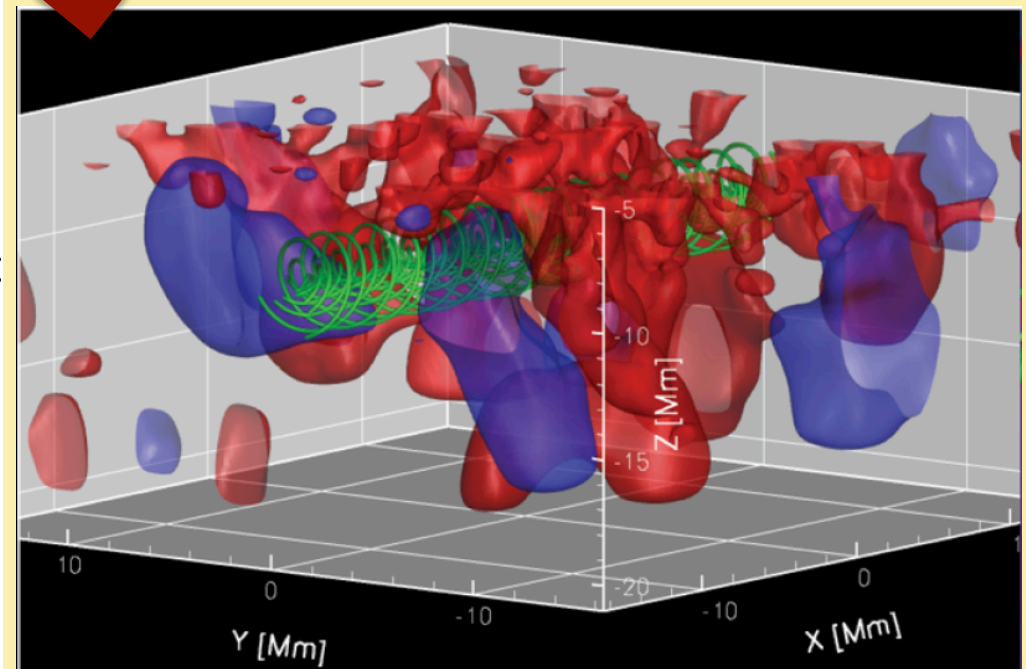


Magnetic Flux Emergence

F. Fang et al., ApJ 754, 15 (2012).



Vertical stratification of density and temperature



Initial flux rope (green rods) at $Z = -10$ Mm, surrounded by convective downflows (blue) and upflows (red)

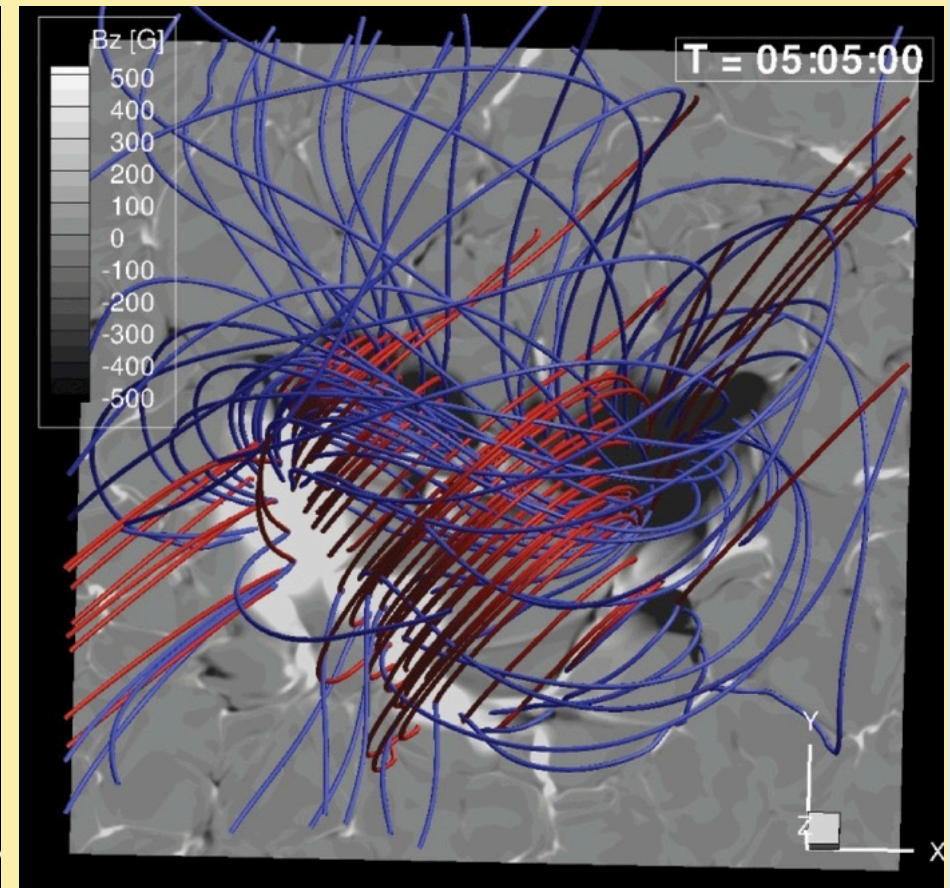
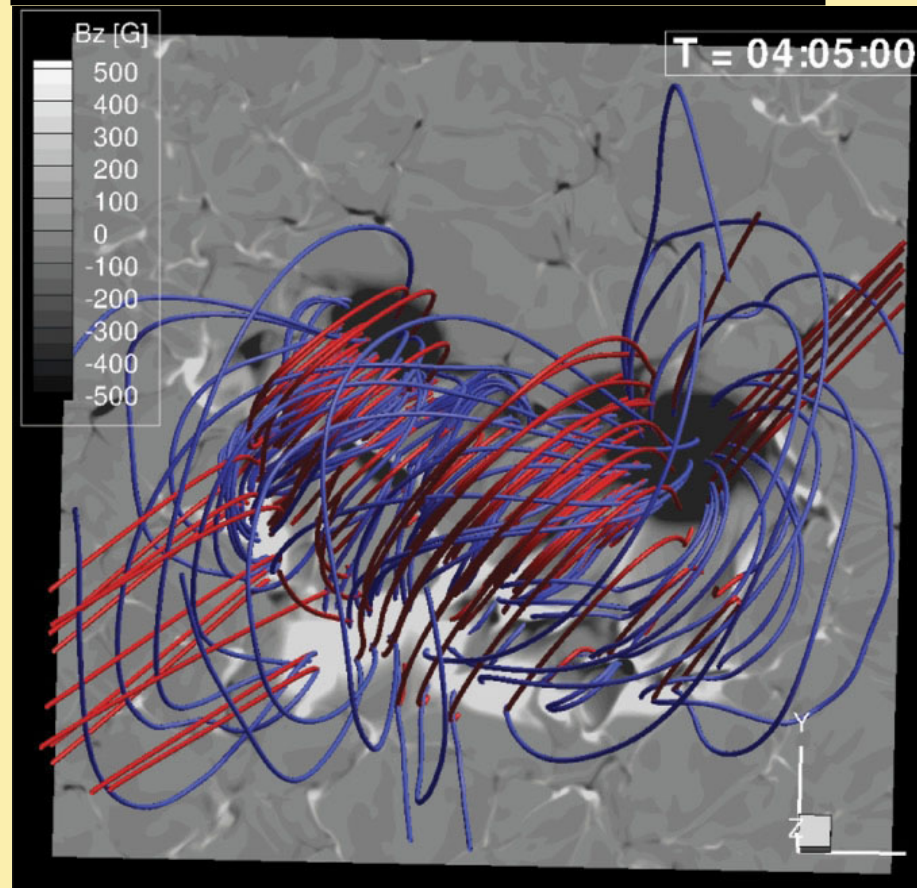
Build-up of Free Energy during Emergence



Plane: Photospheric Bz field

Blue rods: model field

Red rods: potential field



Summary and Outlook



■ AWSOM model for the solar corona and inner heliosphere:

- Alfvén-wave turbulence and three-temperature model
- Validation studies with EUV images and 1AU data shows that this model can capture many features of the solar corona and inner heliosphere

■ AWSOM has just been transferred to CCMC for testing

- We are presently constraining the few model parameters to have good model-data comparison for all Carrington rotations.

■ Arrival time and Bz at 1AU of CMEs using Gibson & Low flux ropes

- Next: automated procedure for flux rope initiation to predict arrival time and Bz

■ Future directions:

- Regional model with MAGIC magnetogram processing suite of tools.
- coupling of flux emergence and regional models with the AWSOM solar wind model. Gabor Toth will present a new coupler that will be used.